Thermally Bianisotropic Metamaterials Induced by Spatial Asymmetry

Gal Shmuel*
Department of Mechanical Engineering, Technion-Israel Institute of Technology, Israel

John R. Willis†
Centre for Mathematical Sciences, Cambridge University
(Dated: July 2, 2025)

Breaking spatial symmetries can induce interactions between disparate physical fields, which manifest in the macroscopic properties of materials as cross-coupling terms. Prominent examples include Willis terms in phononics and bianisotropic terms in photonics. However, the development of analogous cross-couplings in heat conduction remains limited and incomplete; here, we close this knowledge gap. To this end, we introduce an exact and universal homogenization method to capture the macroscopic dynamics of various physical processes in heterogeneous media. For heat conduction and thermodynamics, the method shows that thermal bianisotropy emerges through the intentional design of spatial asymmetry. In certain conditions, the resulting macroscopic description is free from the infinite heat speed paradox inherent in Fourier's law of conduction. We support the exact theory with examples based on heuristic homogenization of a canonical scattering problem. These results may benefit the design of thermal metamaterials with asymmetric response.

Metamaterials are composite materials architectured to exhibit extraordinary effective properties, in value or in nature [1]. A route to calculate and design such properties is via homogenization theories, aimed at extracting the features of materials with internal structure, features that that may be difficult to observe in the exact description [2–7]. Willis [8–11] developed an exact homogenization theory for elastodynamics, revealing several metamaterial features, perhaps the most notable being the unusual macroscopic coupling between momentum and strain. The advent of metamaterials revived interest in this theory [12–17], mainly since these cross-couplings provide additional mechanisms for wave manipulation [18–24].

The applicability of the homogenization framework developed by Willis goes beyond elastodynamics. In electromagnetics, it predicts bianisotropic response, even when constituent materials have no magnetoelectric couplings [25], a conclusion that was obtained by the electromagnetics community using other means [4, 26, 27]). A generalization of the theory by Shmuel and Pernas-Salomón [28] to piezoelectric media led to the discovery of metamaterial coupling between momentum and electric field [29–33], earning the name 'electromomentum coupling'.

Here, we transform these homogenization schemes to heat conduction and thermodynamics aligning with recent interest in thermal metamaterial [34, 35]. This transformation is not trivial, owing to the difference in the equations that govern heat conduction relative to other transport phenomena. Specifically, classical heat conduction is governed by a parabolic-type partial differential equation, whereas the type of equations that govern elastodynamics, electromagnetics and piezoelectricity is hyperbolic. Nevertheless, we find that the unusual cross-couplings appear also in the macroscopic response of thermal media [36], now between heat flux and temperature; and between entropy and temperature gradient.

A closely related coupling was previously introduced by Torrent et al. [37] and Xu et al. [38], who coined the name *thermal Willis coupling*. Our conclusions are different and substantially broader, as we detail next. To do so, we recall that Ref. [38] begins with the statement "*Willis coupling generically stems from bianisotropy or chirality in wave systems. Nevertheless, those schemes are naturally unavailable in diffusion systems described by a single constitutive relation governed by the Fourier law*". With this belief, to realize thermal Willis coupling Refs. [37, 38] modulated the constitutive properties of the medium both in time and space, which is an extremely challenging design task. However, we prove that spatial asymmetry is sufficient and employ Willis' homogenization schemes originally developed for elastodynamics. In doing so, we interpret the relation between entropy and temperature as a constitutive equation; it is this constitutive equation that was missing in Refs. [37, 38]. As a result, we also provide an expression for the mean entropy that is absent in Refs. [37, 38], There is also a difference in the macroscopic heat equation in Ref. [37] and in Ref. [38]. This is an outcome of ambiguity in defining the nonlocal effective relations within their Bloch-Floquet framework. Simply put, since spatial and temporal derivatives become products with wavenumber and frequency, respectively, they are mixed up in their transformed domain [14, 29]. As a result, there are different possibilities to invert the effective relations back into the spatiotemporal domain. Following Fietz and Shvets [39], and Willis [25], here we eliminate this ambiguity by introducing a residual field which acts as additional source [4, 16] and renders the mean field variables independent. Finally, our homogenization is broader in that it applies to three-dimensional media which may be periodic or random, finite or infinite, while the homogenization schemes in Refs. [37, 38] are limited to infinite one-dimensional media modulated in one direction.

Before we proceed to the analysis, we highlight a major implication of our homogenization scheme: in effect, the nature of the heat equation for certain composites is no longer parabolic and terms that are nonlocal in space and time now dictate thermal relaxation. In the spatially-local approxima-

* meshmuel@technion.ac.il
† jrw1005@cam.ac.uk

tion, examples show that these terms can eliminate the unrealistic prediction of infinite speed of thermal signals in classical heat conduction theory. Formulating heat conduction theories with finite speed [40] (so-called second sound [41]) is the focus numerous works which date back to Cattaneo's pioneering paper [42, 43]. Notably, we arrive at a reminiscent result without postulating from the outset a dependency on the history of the temperature; rather, it is an inevitable outcome of our homogenization scheme. We emphasize that, while it is well established that heat can propagate as waves in the phonon hydrodynamic regime at the micrometer scale [44] and in the phonon coherent regime at the nanometer scale [45], there is still no conclusive experimental evidence for macroscopic hyperbolic heat conduction. Interestingly, the studies suggesting such behavior address heterogeneous media [46–48].

We begin by recalling the equations that govern heat conduction. Using Gibbs relations, we write the energy balance equation as

$$\theta_{\mathrm{R}}\dot{\eta} + \nabla \cdot \mathbf{q} = r, \tag{1}$$

where η and r are the entropy and heat source per unit volume, respectively, $\mathbf{q}$ is the heat flux per unit area and θ_{R} is the reference temperature. Fourier's law, $\mathbf{q} = -\boldsymbol{\kappa}\nabla\theta$, states that $\mathbf{q}$ is coupled with the gradient temperature change $\nabla\theta$ by the thermal conductivity tensor $\boldsymbol{\kappa}$. In addition, the temperature and entropy are coupled by the specific heat c such that $\theta_{\mathrm{R}}\eta = c\theta$. Recognizing the latter as a constitutive equation is key to transforming Willis' homogenization method [25] from electromagnetics and elastodynamics to heat conduction. We provide complete details of the scheme in a companion paper [49], and here summarize its key principles and main results. The method uses ensemble averaging in order to define the effective fields [50], such that they satisfy identically the macroscopic equations. The method also employs a residual kinematic field which delivers a unique definition of effective relations. After some work using Green's functions and adjoint equations, we are able to express the effective heat flux and entropy in terms of the effective temperature and its gradient. These effective relations are nonlocal in space and time and take bianisotropic form

$$\begin{pmatrix} -\langle \mathbf{q} \rangle \\ \langle \theta_{\mathrm{R}}\eta \rangle \end{pmatrix} = \begin{pmatrix} \tilde{\boldsymbol{\kappa}} & \tilde{\boldsymbol{\chi}} \\ \tilde{\boldsymbol{\xi}} & \tilde{c} \end{pmatrix} \begin{pmatrix} \langle \nabla\theta - \boldsymbol{\zeta} \rangle \\ \langle \theta \rangle \end{pmatrix}, \tag{2}$$

where $\langle\cdot\rangle$ denotes ensemble averaging, $\boldsymbol{\zeta}$ is the residual temperature gradient that enables the derivation of a unique set of physically meaningful effective properties [25, 31, 39], and $\tilde{\boldsymbol{\chi}}$ and $\tilde{\boldsymbol{\xi}}$ are bianisotropic vector terms that are absent from the microscopic constitutive relations. The structure of the kernel in Eq. (2) suggests the following alternative form

$$\begin{aligned} \begin{pmatrix} -\langle \mathbf{q} \rangle \\ \langle \theta_{\mathrm{R}}\eta \rangle \end{pmatrix} = & \begin{pmatrix} \langle \boldsymbol{\kappa} \rangle & \mathbf{0} \\ \mathbf{0} & \langle c \rangle \end{pmatrix} \begin{pmatrix} \langle \nabla\theta - \boldsymbol{\zeta} \rangle \\ \langle \theta \rangle \end{pmatrix} \\ & + \begin{pmatrix} \hat{\boldsymbol{\kappa}} & \hat{\boldsymbol{\xi}}^{\dagger} \\ \hat{\boldsymbol{\xi}} & \hat{c} \end{pmatrix} \begin{pmatrix} \langle \nabla\theta - \boldsymbol{\zeta} \rangle \\ \langle \dot{\theta} \rangle \end{pmatrix}, \end{aligned} \tag{3}$$

where $\hat{\boldsymbol{\xi}}$ and $\hat{\boldsymbol{\xi}}^{\dagger}$ are an adjoint pair if the microscopic relations are self-adjoint. To demonstrate the implication of Eq. (2) in the simplest way, we substitute its local limit in the one-dimensional case into the macroscopic heat equation, and then set $\zeta = 0$ [51]. We obtain

$$\tilde{\kappa}\partial_x^2 \langle\theta\rangle = \hat{c}\,\partial_t^2 \langle\theta\rangle + \langle c \rangle \partial_t \langle\theta\rangle + \left(\hat{\xi} - \hat{\xi}^{\dagger}\right) \partial_{xt} \langle\theta\rangle . \tag{4}$$

In some of the examples that we provide $\hat{c} > 0$, suggesting that certain compositions, at specific frequencies, transmit thermal fields with a finite speed.. In the local limit of a reciprocal solid, the contributions of the bianisotropic terms cancel each other out in the wave equation since $\hat{\xi} = \hat{\xi}^{\dagger}$, and the equation takes the form of the Telegrapher's equation [52]. Nevertheless, the cross-couplings still modify the thermal impedance $Z = \theta/q$ and thus break the symmetry of heat conduction. Specifically, the characteristic thermal impedance in the $\pm x$ direction in the presence of a heat source with time-dependency $e^{i\omega t}$ is

$$Z^{\pm} = \left(\mp\tilde{k}\tilde{\kappa} - i\omega\tilde{\xi}\right)^{-1}, \tag{5}$$

where $\tilde{k} = \sqrt{i\omega\tilde{c}/\tilde{\kappa}}$ and evidently $\tilde{\xi}$ introduces a direction-dependent phase shift. Measurement techniques which rely on periodic heating and depend on the thermal impedance, such as the 3ω method [53, 54], can therefore serve as tool for quantifying $\tilde{\xi}$ experimentally.

Motivated by the insights gained by the exact homogenization method, we proceed to quantify this symmetry breaking in a 1D scattering problem and develop a heuristic homogenization scheme in the long-wavelength limit, when the thermal wavelength owing to periodic heating [55] is much larger than the size of the scatterer. To this end, we consider a setting in which the heterogeneous medium acts as the thermal scatterer in-between two homogeneous semi-infinite slabs with specific heat c_0 and thermal conductivity κ_0 (Fig. 1). The slabs support leftward- and rightward evanescent solutions of the form $\theta(x,t) = \Theta(x)\, e^{i\omega t}$, where

$$\Theta(x) = \begin{cases} a_{\mathrm{L}}^{-} e^{k_0(x+l/2)} + a_{\mathrm{L}}^{+} e^{-k_0(x-l/2)}, & x \le -l/2, \\ a_{\mathrm{R}}^{-} e^{k_0(x+l/2)} + a_{\mathrm{R}}^{+} e^{-k_0(x-l/2)}, & x \ge l/2, \end{cases} \tag{6}$$

$k_0 = \sqrt{i\omega c_0/\kappa_0}$ is the wavenumber and some of the coefficients $\{a_{\mathrm{L,R}}^{\pm}\}$ may vanish, depending on the excitation.

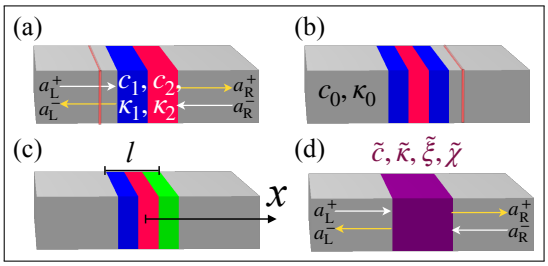

Figure 1. Heterogeneous scatterers in-between two homogeneous semi-infinite slabs. Red lines in panels (a) and (b) denote planar heat sources at the left- and right slabs (d). Homogeneous scatterer with effective bianisotropic terms that generates that same scattering response as the heterogeneous scatterer.

Specifically, if the only heat source is within the finite medium, then $a_{\rm L}^+$ and $a_{\rm R}^-$ must vanish for the temperature to be finite at $\pm\infty$. However, if heat sources exist in the semi-infinite slabs, $a_{\rm L}^+$ and $a_{\rm R}^-$ admit nonzero values owing to incoming heat from the sources to the scatterer. In any case, the continuity of the temperature and heat flux at the interfaces between the slabs and the scatterer couples $\mathsf{a}_{\rm L} = \left(a_{\rm L}^+, a_{\rm L}^-\right)^T$ and $\mathsf{a}_{\rm R} = \left(a_{\rm R}^+, a_{\rm R}^-\right)^T$ by the scattering matrix K. We detail the derivation of its components in the companion paper [49], noting here that K has the form

$$\mathsf{K} = \begin{pmatrix} t_{\rm L} - r_{\rm R} t_{\rm R}^{-1} r_{\rm L} & r_{\rm R} t_{\rm R}^{-1} \\ -r_{\rm L} t_{\rm R}^{-1} & t_{\rm R}^{-1} \end{pmatrix}, \tag{7}$$

such that $r_{\rm L}$ and $t_{\rm L}$ ($r_{\rm R}$ and $t_{\rm R}$) are the reflection and transmission coefficients owing to a source in the left (right) slab, respectively. We note that several methods such as thermal wave interferometry experimental technique for extracting thermal properties rely on measurements of these reflection coefficients owing to periodic heating [56]. We find that $t_{\rm L} = t_{\rm R}$ as reciprocity requires, however $r_{\rm L} \neq r_{\rm R}$; it is this asymmetry that is captured by the effective bianisotropic terms, as we show in the numerical examples to follow.

Our heuristic homogenization aims at replacing the heterogeneous scatterer by a fictitious homogeneous medium that generates the same measurable fields, that is the same scattering matrix K. At the outset, we note that since K has three independent components ($r_{\rm L}, r_{\rm R}$ and $t_{\rm L} \equiv t_{\rm R}$), any attempt to reproduce it using standard constitutive relations with only two material parameters (c and κ) will inevitably lead to inconsistencies. To proceed with the homogenization process, we derive the transfer matrix that relates the temperature and heat flux at both ends of a fictitious bianisotropic medium, which is governed by the local form of Eq. (2). We obtain the following expressions for the effective properties by requiring that the transfer matrix of the bianisotropic medium matches that of the heterogeneous scatterer:

$$\tilde{\kappa} = M_{12}^{-1}, \tilde{c} = -\frac{\det \mathsf{M}}{i\omega M_{12}}, \tilde{\xi} = \frac{M_{22}}{i\omega M_{12}}, \tilde{\chi} = -\frac{M_{11}}{M_{12}}, \tag{8}$$

where the transfer matrix of the heterogeneous scatterer is $\mathsf{T} = e^{\mathsf{M}l}$. Since $\det \mathsf{T} = 1$, it follows that $\mathrm{tr}\, \mathsf{M} = 0$ and hence $\tilde{\chi} = i\omega\tilde{\xi}$.

We proceed to evaluate numerical examples using materials and thicknesses that were used in related studies of periodic heat diffusion in layered solids, see Ref. [57] for the material parameters. We begin with a bilayer made of SiO_2 and diamond, each layer having thickness 25 nm [Fig. 1(a)]. Fig. 2 shows the effective properties in the frequency domain calculated with Eq. (8), recalling that this frequency-dependent nature of the homogenized model is a manifestation of the temporal nonlocal nature of the effective response [1]. We observe that $\tilde{\kappa}$ and $\tilde{c}$ are complex-valued functions that recover the harmonic- and arithmetic means, respectively, in the low-frequency limit. Both the real- and imaginary parts of these effective functions increase with frequency. The parameter $\hat{c}$ is obtained by subtracting from $\tilde{c}$ the arithmetic mean of c. The real part of $\hat{c}$ is an even function. It is of order ω^2 as $\omega \to 0$, reducing to a linear dependence at larger frequency. It contributes a modest amount of dispersion. The imaginary part of $\hat{c}$ is very closely proportional to ω, corresponding to the second derivative of $\langle\theta\rangle$ in Eq. (4). Importantly, $\tilde{\chi}$ is purely imaginary and equal to $i\omega\tilde{\xi}$. For the entire range of frequency plotted, $\tilde{\xi}$ is constant and thus $\tilde{\chi}$ is linear in ω.

The second example considers symmetric trilayer made of a diamond layer in-between two SiO_2 layers, where the thickness of each layer is 16.67 nm [Fig. 1(b)]. Fig. 3 mirrors Fig. 2, now for the trilayer. Here again, $\tilde{\kappa}$ and $\tilde{c}$ are complex functions which recover the harmonic and arithmetic means, respectively, in the low-frequency limit. However, the imaginary part of $\hat{c}$ is negative at small ω. It displays a minimum around 3 G rad/s and thereafter increases. We have confirmed that this increase is linear in ω over a substantial range beyond the minimum, which is sufficient to deliver to a good approximation of the second derivative term in Eq. (4), with the lower frequencies contributing to the dissipation. Notably, $\tilde{\chi}$ and $\tilde{\xi}$ are identically zero, as expected due to the symmetry of the scatterer. The effective properties in Fig. 4 are obtained by replacing the material of the left layer with copper [Fig. 1(c)], a symmetry breaking that yields nonzero $\tilde{\chi}$ and $\tilde{\xi}$, like in Fig. 2. Cross-coupling terms of the asymmetric trilayer are greater than those of the bilayer, demonstrating that it is possible to optimize thermal bianisotropy by microstructure design.

The magnitude of $\tilde{\xi}$ is directly related to the asymmetry in the reflection properties. To illustrate this relation, we plot in Fig. 5 the magnitude ratio and phase difference between between the reflection coefficients ($r_{\rm L}$ and $r_{\rm R}$) as functions of frequency, for the different scatterers shown Figs. 2-4. We observe that a larger magnitude of $\tilde{\xi}$ corresponds to a greater relative phase between $r_{\rm L}$ and $r_{\rm R}$.

To conclude, we have derived a formal expression for the effective response of heat-conducting composites, showing that this response inevitably must display thermal bianisotropy, and have supported this observation with simple examples based on heuristic homogenization of subwavelength elements in canonical gedanken scattering experiments. These examples demonstrate that thermal bianisotropy manifests as an asymmetry in the thermal reflection coefficients, which can be experimentally measured using the thermal wave interferometry technique. Our analysis also sug-

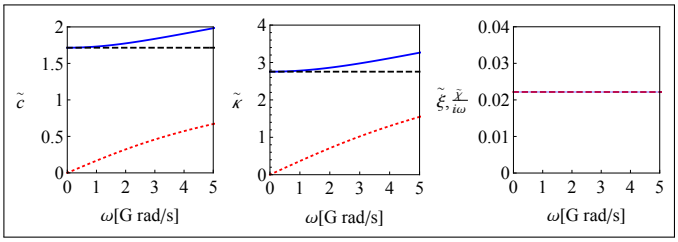

Figure 2. Effective (a) specific heat and (b) thermal conductivity properties of a bilayer made of SiO_2 and diamond [Fig. 1(a)]. Solid blue and dashed red curves denote real and imaginary parts, respectively. Dashed black lines denote the harmonic and arithmetic means. (c) Effective bianisotropic terms $\tilde{\xi}$ (dashed red) and $\tilde{\chi}/i\omega$ (solid blue).

gests that the effective heat transport in certain composites, at specific frequencies, is hyperbolic. To date, there is no conclusive experimental evidence for macroscopic hyperbolic heat conduction; however, the works that do suggest such behavior study heterogeneous media. Our homogenization process thus proposes a thermal metamaterial that exhibits macroscopic heat transport not found in nature. Undoubtedly, the internal geometry of the metamaterial plays a major role in determining its bianisotropic effect. This is consistent with numerous findings in other fields of physics, where cross-couplings are shown to be maximized by adjusting the layer thicknesses [32, 58, 59], and more generally, by altering the geometry of the scatterer in higher dimensions [22, 60]. Similar to how experimentally verified metamaterials exhibiting and maximizing Willis couplings [21, 60, 61] followed their theoretical discovery [8, 10, 25], our analysis opens the avenue for experimental realizations of their thermal counterparts. It also sets the stage for our future work on thermomomentum Willis-type couplings in thermoelastic materials, which mirror the electromomentum effect in piezoelectric materials.

We thank the editor and reviewers for their valuable feedback, which has helped us improve this letter. G.S. thanks Profs. Oleg Gendelman and Beni Cukurel for fruitful discussions, and funding by the European Union (ERC, EXCEPTIONAL, Project No. 101045494). Funded by the European Union. Views and opinions expressed are however those of the author(s) only and do not necessarily reflect those of the European Union or the European Research Council Executive Agency. Neither the European Union nor the granting authority can be held responsible for them.

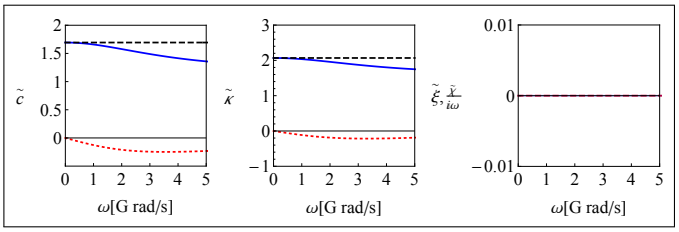

Figure 3. Effective properties of a symmetric trilayer made of a diamond layer in-between two SiO_2 layers [Fig. 1(b)]. Legend same as in Fig. 2. The bianisotropic terms are null, owing to the symmetry of the scatterer.

[1] Muamer Kadic, Tiemo Bückmann, Robert Schittny, and Martin Wegener. Metamaterials beyond electromagnetism. *Reports on Progress in Physics*, 76(12):126501, 2013.

[2] C. R. Simovski. Material parameters of metamaterials (a review). *Optics and Spectroscopy*, 107(5):726, 2009.

[3] C. Fietz and G. Shvets. Metamaterial homogenization: extraction of effective constitutive parameters. *Proc. SPIE 7392, Metamaterials: Fundamentals and Applications II*, page 73920L, 2009.

[4] Andrea Alù. First-principles homogenization theory for periodic metamaterials. *Phys. Rev. B*, 84:075153, Aug 2011.

[5] Biswajit Banerjee. *An introduction to metamaterials and waves in composites*. CRC Press, 2011.

[6] Ankit Srivastava. Elastic metamaterials and dynamic homogenization: a review. *International Journal of Smart and Nano Materials*, 6(1):41–60, 2015.

[7] Muamer Kadic, Graeme W. Milton, Martin van Hecke, and Martin Wegener. 3d metamaterials. *Nature Reviews Physics*, 1(3):198–210, 2019.

[8] J R Willis. Variational principles for dynamic problems for inhomogeneous elastic media. *Wave Motion*, 3(1):1–11, 1981.

[9] J R Willis. The nonlocal influence of density variations in a composite. *Int. J. Solids Struct.*, 21(7):805–817, 1985.

[10] J R Willis. Continuum Micromechanics. chapter Dynamics of Composites, pages 265–290. Springer-Verlag New York, Inc., New York, NY, USA, 1997.

[11] John R. Willis. The construction of effective relations for waves in a composite. *Comptes Rendus Mécanique*, 340(4):181 – 192, 2012. Recent Advances in Micromechanics of Materials.

[12] Michael B Muhlestein, Caleb F Sieck, Andrea Alù, and Michael R Haberman. Reciprocity, passivity and causality in Willis materials. *Proc. R. Soc. London A Math. Phys. Eng. Sci.*, 472(2194), 2016.

[13] A. L. Shuvalov, A. A. Kutsenko, A. N. Norris, and O Poncelet. Effective Willis constitutive equations for periodically stratified anisotropic elastic media. *Proc. R. Soc. London A Math. Phys. Eng. Sci.*, 467(2130):1749–1769, 2011.

[14] Hussein Nassar, Qi-Chang He, and Nicolas Auffray. Willis elastodynamic homogenization theory revisited for periodic media. *Journal of the Mechanics and Physics of Solids*, 2015.

[15] H Nassar, Q.-C. He, and N Auffray. On asymptotic elastodynamic homogenization approaches for periodic media. *J. Mech. Phys. Solids*, 88:274–290, 2016.

[16] Caleb F Sieck, Andrea Alù, and Michael R Haberman. Origins of Willis coupling and acoustic bianisotropy in acoustic metamaterials through source-driven homogenization. *Phys. Rev. B*, 96(10):104303, 2017.

[17] Shixu Meng and Bojan B Guzina. On the dynamic homogenization of periodic media: Willis' approach versus two-scale paradigm. *Proc. R. Soc. London A Math. Phys. Eng. Sci.*, 474(2213), 2018.

[18] Steven R. Craig, Bohan Wang, Xiaoshi Su, Debasish Banerjee, Phoebe J. Welch, Mighten C. Yip, Yuhang Hu, and Chengzhi Shi. Extreme material parameters accessible by active acoustic metamaterials with Willis coupling. *The Journal of the Acoustical Society of America*, 151(3):1722–1729, 03 2022.

[19] Joshua Lau, Suet To Tang, Min Yang, and Zhiyu Yang. Coupled

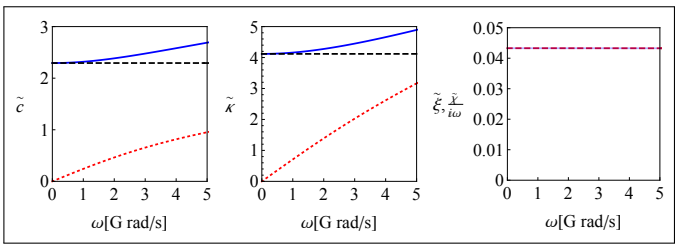

Figure 4. Effective properties of a trilayer made of SiO_2, diamond and copper layers [Fig. 1(c)]. Legend same as in Fig. 2.

Decorated Membrane Resonators with Large Willis Coupling. *Phys. Rev. Applied*, 12:014032, Jul 2019.

[20] Aurélien Merkel, Vicent Romero-García, Jean-Philippe Groby, Jensen Li, and Johan Christensen. Unidirectional zero sonic reflection in passive $\mathcal{PT}$-symmetric Willis media. *Phys. Rev. B*, 98:201102, Nov 2018.

[21] Michael B. Muhlestein, Caleb F. Sieck, Preston S. Wilson, and Michael R. Haberman. Experimental evidence of Willis coupling in a one-dimensional effective material element. *Nature Communications*, 8:15625 EP –, 06 2017.

[22] Li Quan, Younes Ra'di, Dimitrios L Sounas, and Andrea Alù. Maximum Willis Coupling in Acoustic Scatterers. *Phys. Rev. Lett.*, 120(25):254301, 2018.

[23] Junfei Li, Ailing Song, and Steven A. Cummer. Bianisotropic acoustic metasurface for surface-wave-enhanced wavefront transformation. *Phys. Rev. Applied*, 14:044012, Oct 2020.

[24] Xiaoshi Su and Andrew N. Norris. Retrieval method for the bianisotropic polarizability tensor of willis acoustic scatterers. *Phys. Rev. B*, 98:174305, Nov 2018.

[25] J R Willis. Effective constitutive relations for waves in composites and metamaterials. *Proc. R. Soc. London A Math. Phys. Eng. Sci.*, 467(2131):1865–1879, 2011.

[26] Ricardo Marqués, Francisco Medina, and Rachid Rafii-El-Idrissi. Role of bianisotropy in negative permeability and left-handed metamaterials. *Phys. Rev. B*, 65:144440, Apr 2002.

[27] Andrea Alù. Restoring the physical meaning of metamaterial constitutive parameters. *Phys. Rev. B*, 83:081102, Feb 2011.

[28] René Pernas-Salomón and Gal Shmuel. Symmetry breaking creates electro-momentum coupling in piezoelectric metamaterials. *Journal of the Mechanics and Physics of Solids*, 134:103770, 2020.

[29] René Pernas-Salomón and Gal Shmuel. Fundamental principles for generalized Willis metamaterials. *Phys. Rev. Applied*, 14:064005, Dec 2020.

[30] René Pernas-Salomón, Michael R. Haberman, Andrew N. Norris, and Gal Shmuel. The electromomentum effect in piezoelectric Willis scatterers. *Wave Motion*, page 102797, 2021.

[31] Alan Muhafra, Majd Kosta, Daniel Torrent, René Pernas-Salomón, and Gal Shmuel. Homogenization of piezoelectric planar Willis materials undergoing antiplane shear. *Wave Motion*, 108:102833, 2022.

[32] Majd Kosta, Alan Muhafra, Rene Pernas-Salómon, Gal Shmuel, and Oded Amir. Maximizing the electromomentum coupling in piezoelectric laminates. *International Journal of Solids and Structures*, 254-255:111909, 2022.

[33] Kevin Muhafra, Michael R. Haberman, and Gal Shmuel. Discrete one-dimensional models for the electromomentum coupling. *Phys. Rev. Appl.*, 20:014042, Jul 2023.

[34] Ying Li, Wei Li, Tiancheng Han, Xu Zheng, Jiaxin Li, Baowen Li, Shanhui Fan, and Cheng-Wei Qiu. Transforming heat transfer with thermal metamaterials and devices. *Nature Reviews Materials*, 6(6):488–507, 2021.

[35] Zeren Zhang, Liujun Xu, Teng Qu, Min Lei, Zhi-Kang Lin, Xiaoping Ouyang, Jian-Hua Jiang, and Jiping Huang. Diffusion metamaterials. *Nature Reviews Physics*, 5(4):218–235, 2023.

[36] Here, the macroscale refers to the scale of the entire body, where it can be analyzed as a homogeneous continuum with effective properties, while microscale corresponds to the typical dimensions of the constituents [50].

[37] Daniel Torrent, Olivier Poncelet, and Jean-Chirstophe Batsale. Nonreciprocal thermal material by spatiotemporal modulation. *Phys. Rev. Lett.*, 120:125501, Mar 2018.

[38] Liujun Xu, Guoqiang Xu, Jiaxin Li, Ying Li, Jiping Huang, and Cheng-Wei Qiu. Thermal Willis coupling in spatiotemporal diffusive metamaterials. *Phys. Rev. Lett.*, 129:155901, Oct 2022.

[39] Chris Fietz and Gennady Shvets. Current-driven metamaterial homogenization. *Physica B: Condensed Matter*, 405(14):2930 – 2934, 2010. Proceedings of the Eighth International Conference on Electrical Transport and Optical Properties of Inhomogeneous Media.

[40] Morton E. Gurtin and A. C. Pipkin. A general theory of heat conduction with finite wave speeds. *Archive for Rational Mechanics and Analysis*, 31(2):113–126, 1968.

[41] D. S. Chandrasekharaiah. Thermoelasticity with Second Sound: A Review. *Applied Mechanics Reviews*, 39(3):355–376, 03 1986.

[42] Carlo Cattaneo. Sulla conduzione del calore. *Atti Sem. Mat. Fis. Univ. Modena*, 3:83–101, 1948.

[43] Gianfranco Capriz, Krzysztof Wilmanski, and Paolo Maria Mariano. Exact and approximate maxwell-cattaneo-type descriptions of heat conduction: A comparative analysis. *International Journal of Heat and Mass Transfer*, 175:121362, 2021.

[44] Y. Guo and M. Wang. Phonon hydrodynamics and its applications in nanoscale heat transport. *Physics Reports*, 595:1–44, 2015.

[45] Zhongwei Zhang, Yangyu Guo, Marc Bescond, Jie Chen, Masahiro Nomura, and Sebastian Volz. Heat conduction theory including phonon coherence. *Physical Review Letters*, 128(1):015901, jan 2022.

[46] W. Kaminski. Hyperbolic heat conduction equation for materials with a nonhomogeneous inner structure. *Journal of Heat Transfer*, 112(3):555–560, 08 1990.

[47] S. L. Sobolev. Heat conduction equation for systems with an inhomogeneous internal structure. *Journal of Engineering Physics and Thermophysics*, 66(4):436–440, 1994.

[48] K. Mitra, S. Kumar, A. Vedavarz, and M. K. Moallemi. Experimental evidence of hyperbolic heat conduction in processed meat. *Journal of Heat Transfer*, 117(3):568–573, August 1995.

[49] Gal Shmuel and John R. Willis. An exact homogenization method in heat conduction. *To be submitted to Phy. Rev. Appl.*

[50] Zvi Hashin. Analysis of composite materialsÑa survey. *Journal of Applied Mechanics*, 50(3):481–505, 1983.

[51] The local limit of the Willis equations is referred to as the Milton-Briane-Willis equations [62], at which we can identify the bianisotropic terms without needing a residual field [30, 63].

[52] J.A. Buck and W.H. Hayt. *Engineering Electromagnetics*. McGraw-Hill Education, 2011.

[53] David G. Cahill. Thermal conductivity measurement from 30 to 750k: the 3ω method. *Review of Scientific Instruments*,

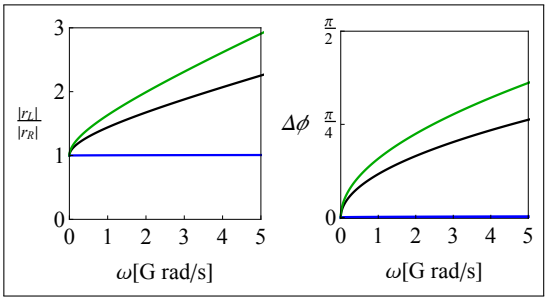

Figure 5. Magnitude ratio (left panel) and phase difference (right panel curves) between between the reflection coefficients (r_{L} and r_{R}) as functions of frequency, for the different scatterers shown in Figs. 2 (black), 3 (blue) and 4 (green).

61(2):802–808, February 1990.

[54] J. J. Martínez-Flores, L. Licea-Jiménez, S. A. Pérez García, J. Rodríguez-Viejo, and J. Alvarez-Quintana. Comprehensive characterization of thermophysical properties in solids using thermal impedance. *Journal of Applied Physics*, 112(9):094901, 2012.

[55] H. S. Carslaw and J. C. Jaeger. *Conduction of Heat in Solids*. Oxford University Press, Oxford, 2nd edition, 1959.

[56] C. A. Bennett and R. R. Patty. Thermal wave interferometry: a potential application of the photoacoustic effect. *Appl. Opt.*, 21(1):49–54, Jan 1982.

[57] Tao Li and Zhen Chen. Scattering matrix formalism to model periodic heat diffusion in stratified solid media. *Journal of Applied Physics*, 132(12):125103, 2022.

[58] Zhizhou Zhang, Jeong-Ho Lee, and Grace X. Gu. Rational design of piezoelectric metamaterials with tailored electromomentum coupling. *Extreme Mechanics Letters*, 55:101785, 2022.

[59] Hai D. Huynh, S.S. Nanthakumar, Harold S. Park, Timon Rabczuk, and Xiaoying Zhuang. The effect of electromomentum coupling on unidirectional zero reflection in layered generalized willis metamaterials. *Extreme Mechanics Letters*, 77:102318, 2025.

[60] Anton Melnikov, Yan Kei Chiang, Li Quan, Sebastian Oberst, Andrea Alù, Steffen Marburg, and David Powell. Acoustic meta-atom with experimentally verified maximum Willis coupling. *Nature Communications*, 10(1):3148, 2019.

[61] Yongquan Liu, Zixian Liang, Jian Zhu, Lingbo Xia, Olivier Mondain-Monval, Thomas Brunet, Andrea Alù, and Jensen Li. Willis metamaterial on a structured beam. *Phys. Rev. X*, 9:011040, Feb 2019.

[62] G W Milton, M Briane, and J R Willis. On cloaking for elasticity and physical equations with a transformation invariant form. *New J. Phys.*, 8(10):248, 2006.

[63] Graeme W. Milton. A unifying perspective on linear continuum equations prevalent in physics. part iv: Canonical forms for equations involving higher order gradients. *arXiv: Mathematical Physics*, 2020.